SME Annual Meeting
Feb. 25 - 28, 2018, Minneapolis, MN

Preprint 18-077

COMPUTATIONAL FLUID DYNAMICS MODELING OF DUST CAPTURE BY A NON-CLOGGING SCREEN SYSTEM FOR A FLOODED-BED DUST SCRUBBER

O. A. Velasquez, Univ. of Kentucky, Lexington, KY
A. R. Kumar, Univ. of Kentucky, Lexington, KY
S. Schafrik, Univ. of Kentucky, Lexington, KY
W. C. Wedding, Univ. of Kentucky, Lexington, KY

ABSTRACT

Dust generated on underground mechanized coal mining faces is a health and safety hazard. Continuous miners deployed underground usually have an integrated flooded-bed dust scrubber mounted onto the machine that arrests the generated dust from close to the face and cleanses the air around it. However, the impingement screen might get clogged depending on the coal seam being worked. This necessitates the cleaning of the screen which in turn, reduces the overall availability of the scrubber and, hence the continuous miner.

A novel non-clogging screen has been developed at the Department of Mining Engineering, University of Kentucky. The proposed impingement screen is built up of three individual aluminum screen units 1.5 mm thick and separated by 3 and 2 mm respectively. The screens have long vertical slits measuring 6 mm. A water spray continuously keeps the screen wet and provides for the filter element to arrest the dust particles. The slits force the dust-laden air to make sharp turns. The dust particles cannot change directions rapidly, impact one of the three screens and are separated out based on their momentum. Preliminary computational fluid dynamics (CFD) models have indicated significant cleaning efficiencies in the respirable range at the expense of much lower pressure drops. Results indicated by CFD models and supported by laboratory experiments have been discussed in this paper.

ACKNOWLEDGEMENT

The authors acknowledge the National Institute for Occupational Safety and Health (NIOSH) for funding this research. Dr. Thomas Novak, Professor of Mining Engineering, is also acknowledged for his continued support and encouragement.

INTRODUCTION

Continuous miners are ubiquitous in coal mining around the world. The miners are operated against bling headings, ensuring adequate flow of air at the face could be difficult. The minimum requirement of ventilation airflow quantities at those coal faces are legislated to dilute dust generated to harmless levels. New dust rules promulgated recently have further called for lower exposure levels of personnel working underground (Courtney) (MSHA, 2014) (NIOSH, 2010). Water sprays are also installed at strategic locations and serve as powerful air-movers. The sprays capture some amount of dust generated while cutting. In addition to this, usually, all continuous miners are equipped with a flooded-bed dust scrubber as shown in Figure 1 to capture the dust from close to the extraction drum (Chao & De-sheng, 2000) (Wala, Vytla, Huang, & Taylor, 2008) (Organiscak & Beck, 2010).

These scrubbers are usually powered by a vane-axial flow fan and arrest dust particles on an impingement screen. The screen is kept flooded with water which increases the probability of the particles being captured. A demister installed downstream removes the spent dirty water from the air-stream and forces it to get accumulated in a sump at the bottom of the scrubber system. Clean air is discharged at the back of the continuous miner and away from the coal-face (Gillies., 1982) (Colinet, Reed, & Potts, 2014). An efficient dust scrubbing system could also assist extended cuts (A.M.Wala, J.C.Yingling, & Zhang, 1998).

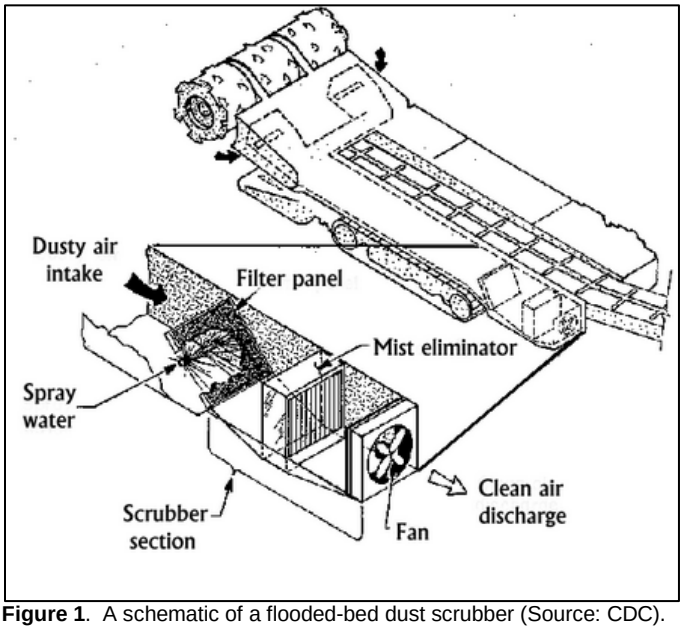

Figure 1. A schematic of a flooded-bed dust scrubber (Source: CDC).

The flooded-bed dust-scrubbers have been proven to be effective in capturing the dust particles, the impingement screen is prone to clogging depending on the coal seam being worked. Clogs increase the resistance of the scrubber system, and decrease the quantity of air processed, greatly impairing efficiency (Kissell & Goodman, 2003). Therefore, even though the cleaning efficiency of the scrubber is improved, the capture efficiency is reduced, and the overall operational efficiency of the scrubbing system goes down. This paper describes a new non-clogging, impingement screen system has been proposed by the authors. Computational fluid dynamics (CFD) models have been set up to mimic the flows and capture of dust particles. Laboratory experiments have been set up to establish the flow-pressure curve. This paper summarizes the performance of the screen system using this numerical modeling approach. Preliminary physical testing of pressure drops through the screen system is discussed in the following section.

DESIGN OF THE SCREEN SYSTEM

The new screen operates similarly to an inertial impactor. The system is made of three individual screens with long parallel slits measuring 6 mm in width as shown in Figure 2. The first and the third screens are identical to each other. The second screen has its slits displaced by 6 mm in the plane of the screen itself. This makes the screen system blind to straight flows. The dust-laden air is forced to make sharp turns at all the screens. This also ensures that there is a near-perfect split of air-flows at all the screens. The design was

conceptualized after an iterative procedure where the screens were first separated by 6 mm. The separation was reduced in steps of 1 mm. The three screens are spaced by distances of 3 mm and 2 mm respectively following the airflow direction in the final design. This was chosen since the pressure drops began to rise for the same airflow at this separation which in turn indicates, acceleration of airflows.

Figure 2. The proposed impingement screen.

The air, being lighter could negotiate these turns easily. However, the heavier dust particles due to their mass cannot follow the streamlines of air. Unlike the flow through an impingement screen of a conventional flooded-bed scrubber system which acts as a porous medium, the trajectory of particles could be described with utmost certainty. Particles hit the solid surfaces of the screen system, which are kept wet by a water spray, installed upstream of the screen system. The film of water together with the screen serves as the filter element and trap the dust particles, thereby cleansing the dirty air. The spent water could now be recycled back into the system, making this set-up a self-sufficient zero discharge system. Detailed CFD models were developed to arrive at the configuration and the dimensions of the screen. Laboratory experiments were developed to establish the correlation with the CFD models.

COMPUTATIONAL FLUID DYNAMICS (CFD) MODELING

Computational fluid dynamics (CFD) models were set-up in the design phase of the screen to examine the major performance parameters of the screen system. The software SC-Flow, version 13 was used to generate unstructured meshes of polyhedral grid elements. It also has independent modules for preprocessing, solving and post-processing. Simplification of geometry, setting up analysis conditions and mesh-generation were carried out in the pre-processing module. Simulations were run on high-performance computing system available within the department. This was especially useful while running transient state simulations on dense meshes.

A three-dimensional drawing of the screen system was developed on a CAD platform. The drawing was imported in a compatible format into the CFD software, where it was cleaned up for problematic features that could lead to divergence while running the simulations. It was decided to use an imaginary vertical plane passing through the center of the system along the general airflow direction to divide the flow volume into two symmetrical entities. One of these volumes was used for further generating the CFD models to save on computing time and resources. All the surfaces of interest were demarcated, registered and assigned unique names. Boundary conditions included flux with turbulence properties depending on the flows at the inlet and, static pressure at the outlet respectively. Impermeable wall conditions were imparted on all other surfaces, other than the plane of symmetry where the free-slip wall conditions were applied. An octree was generated and refined in the areas of interest to manually place the grid elements and to capture the gradients in pressures and velocities accurately. Three prism layers were inserted with an initial thickness governed by the expected magnitude of velocities around those surfaces to account for the wall functions. A computational mesh composed of polyhedral elements was generated and has been shown in Figure 3. Simulations were run to a threshold residual of 0.0001 for velocities and pressure.

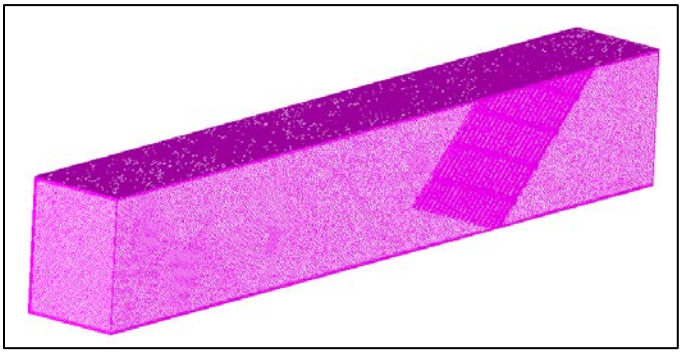

Figure 3. Computational mesh consisting of polyhedral elements.

Mesh independence studies were carried out to establish the objectivity of a parameter with grid sizing. Richardson's method of reporting differences in parameters across meshes was adopted for reporting uncertainty (ASME, 2008). Three different meshes with decreasing size of the mesh cells, h was chosen and magnitudes of velocity, Φ_i at three chosen points in the flow domain were observed. Two of these points were chosen close to the screens. Percentage differences in the absolute values of the magnitude of velocities were calculated. Finally, fine grid convergence indices were calculated with respect to those values. Table 1 shows the results from grid independence studies carried over three meshes with increasing number of mesh elements.

Table 1. Important parameters for grid independence studies.

Parameters	Grid I	Grid II	Grid III
Number of mesh cells, N	912,467	1,829,242	4,114,770
Average height of cell [mm], h	4.66	3.69	2.82
Growth ratio	1.26		1.31
Magnitude of velocity [m/s], Φ_1	5.28	5.27	5.27
Φ_2	5.67	5.51	5.55
Φ_3	5.23	5.23	5.42
Approximate relative errors, %	2.58		0.97
Approximate extrapolated error, %	0.06		0.30
Fine grid convergence index	4.74		3.52

The mesh with about 1.82 million elements was chosen for further processing and analysis after examination of y^+ values on the surfaces. Steady-state simulations were generated to approximate the flows through the system and accompanying pressure drops and hence, to arrive at the system curve. The log files of the primary steady-state simulations were examined to approximate the time it takes for the flow to reach equilibrium. Transient state simulations were then run to track the particles as they travel inside the system. The time-steps have been kept small to adhere to an average Courant number of about 1.00, to prevent any divergence in calculations. Figure 4 shows the plot of Courant number for the flow of 3,000 cfm. Figure 5 shows the magnitude of velocity on a plane parallel to the bottom surface of the ductwork and along the general airflow direction

Then, transient state simulations were developed with the chosen mesh to approximate the particles captured by the screen system. Lagrangian method of particle tracking was adopted to monitor the trajectory of the particles as they moved through the ductwork. The time steps of the transient state simulations were kept at 0.25

milliseconds or lower to ensure that the average Courant number stays close to 1.00. This also ensures that the solver does not diverge.

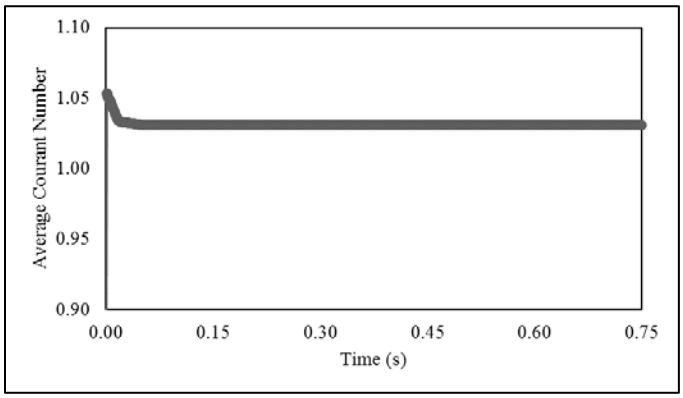

Figure 4. Plot of Courant number for the airflow of 3,000 cfm.

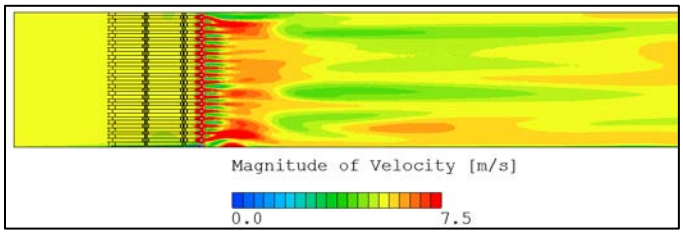

Figure 5. Contours of magnitude of velocity of a plane parallel to the bottom surface.

The particles were assumed to be solid spheres having a density of 1,220 kg/m^3, and the characteristic diameters of the particles were obtained by analyzing the coal sample with an optical particle counter. The particles with average diameters from 1.50 to 14.59 microns were examined. A good estimate of the cleaning efficiency of the screen system could be arrived at using the particle count on the screens since the number of particles generated is known from the CFD program. The particles used in these transient state simulations could mimic the Keystone mineral black 325A coal sample, which was also expected to be used in the laboratory experiments which were being planned at the time of writing this paper.

The particles were released every 0.5 ms at the inlet of the system time until 1,500 cycles of simulations and their trajectory monitored continuously until all the particles escaping are transported out of the system. Assuming that the surface of the screen would be kept wet using the water sprays, the particles were programmed to undergo and perfectly inelastic collision with the three screens. This would mimic the capture of the particles on the flooded screen system. Counters were set up to report particles arriving at each of the screens as well as the outlet and, were classified based on their diameters. The count of the particles reporting at the outlet of the system could be used to calculate the capture efficiency of the screen system. Table 2 shows the relevant analysis conditions pertaining to the particles.

Figure 6 shows the location of the particles colored by the magnitude of their diameters. The percent of particles captured by the screen were obtained from the log files and have been shown in Figure 7. The plot clearly indicates the percent of particles being trapped by the screen increasing with an increase in the flow through the screen system. Capture of lower sized particles is also enhanced with the increase in flows. The impingement screen system is able to capture a significant number of all the particles exceeding about 4 microns in diameter for all airflows.

PRELIMINARY LABORATORY EXPERIMENTS

Experiments were set up in the mine ventilation laboratory to investigate the flows via the impingement screen system. An 8' long duct-work was built with the opening measuring 18" X 12" in dimensions. One end of the duct was connected to a powerful centrifugal fan and the other end was connected to a Dwyer pressure measurement station. This station when equipped with suitable measurement devices could be used to measure the flows and accompanying total and velocity pressures. The fan is operated using a variable frequency drive (VFD) and enables the authors to investigate the performance of the screen over a range of flows. The impingement screen was installed at 45° with the general airflow direction, as a drop-down replacement like the one used in the flooded-bed dust-scrubbers on the continuous miners.

Table 2. Analysis conditions for particle tracking.

Parameters	Values
Flow/ boundary conditions	Flux at the inlet/ outlet, Free slip walls conditions at the plane of symmetry. Smooth impermeable wall conditions at all other surfaces
Time step for transient state simulations	0.25 milliseconds or lower, depending on the incoming airflow speed
Particle type	Solid spherical particles with mass; diameters obtained from the sample to be used for experiments
Density of the particles	1,220 kg/m^3
Count and frequency of particle release	100 particles every 5 cycles, until first 1,500 cycles of transient state simulations
Treatment at walls	Killed at the surfaces of the screens and the outlet
Turbulent diffusion	Considered
Regions to count the particles	Surface of the three screens, outlet

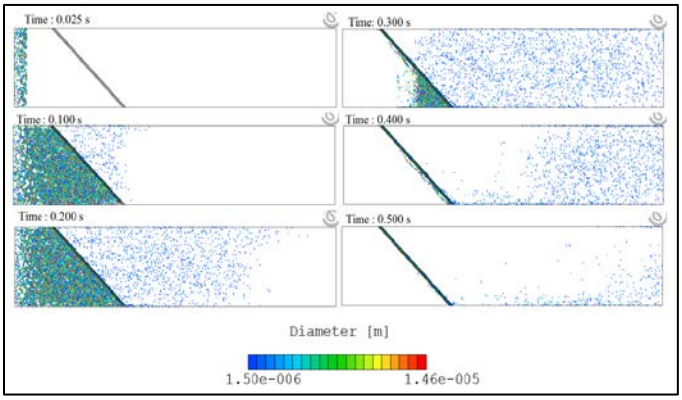

Figure 6. Location of the particles, colored by the magnitude of their diameter.

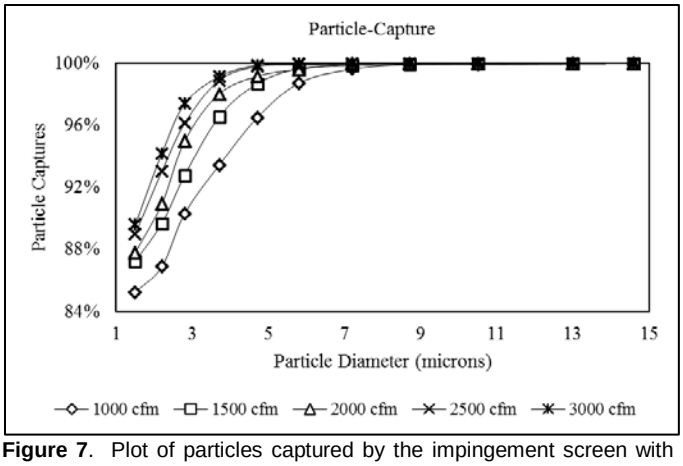

Figure 7. Plot of particles captured by the impingement screen with respect to the airflows.

Experiments were run with the initial frequency set at 10 Hz and velocity and total pressures measured. Frequency was stepped up in steps of 5 Hz until 30 Hz and pressure drops plotted against flows to

obtain the system curve. Figure 8 and Figure 9 show the set-up of the experiments. Figure 10 shows the system curve obtained from the experiments. A plot obtained from CFD models has also been plotted alongside for comparison. The curves show excellent agreement. Total pressure drops obtained towards the regime of higher flows were slightly lower by about 7 % compared to the CFD models, partly due to higher leakages. The system curves obtained from CFD models as well as the laboratory experiments were both observed to follow the Atkinson's equation for flows. The system curves validate the preliminary pressure drops obtained on the CFD models.

Figure 8. Installation of the impingement screen for measurement.

Figure 9. Set-up for the flow measurements

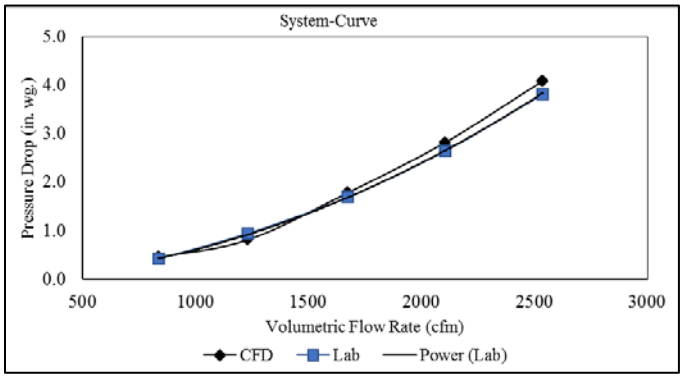

Figure 10. System curves, obtained from the CFD models and laboratory experiments.

CONCLUSIONS AND DISCUSSIONS

This paper describes a novel inertial impactor impingement screen system developed by the authors. The screen is designed to act as an inertial impactor with high flow. Unlike the conventional screen made up of wire meshes, this impingement screen system has three individual screens with long openings running along the length of the screen. Staggered openings make the air change directions rapidly twice and cast dust particles onto the solid surfaces kept wet using water sprays. Because of much wider openings, the screen system is not prone to clogging due to the dust particles generated at the continuous miner face. Preliminary CFD models have shown the screen to capture more than 90 % of the particles by count. The capture efficacy increases with the increase in airflows. Experiments are also being designed to examine the capture of dust particles, using optical particle counters. The screen also shows promise of being scaled to different dimensions provided the native design is kept the same.

FURTHER WORK

Experiments are planned to approximate the cleaning efficacy of the screen system. Figure 11 shows a projected system curve in which the frequency stepped up until 60 Hz. Geometrical scaling of this screen system could also be modeled on CFD software and a prototype constructed to fit in a typical flooded-bed screen housing. This could also be used to test the capture efficacies before proposing implementation on active continuous miners.

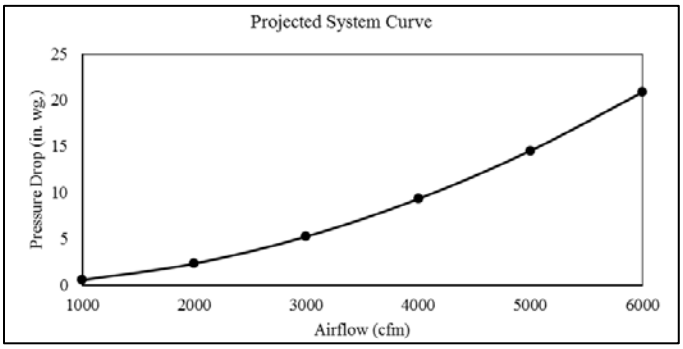

Figure 11. Projected system curve values.

REFERENCES

A.M.Wala, J.C.Yingling, & Zhang, J. (1998). Evaluation of the face ventilation systems for extended cuts with remotely operated mining machines using three-dimensional numerical simulations. *SME Annual Meeting.* Orlando, Florida.

ASME. (2008, July 22). Procedure for Estimation and Reporting of Uncertainty Due to Discretization in CFD Applications. *Journal of Fluids Engineering*. doi:doi:10.1115/1.2960953

Centres for Disease Control and Prevention, National Institute for Occupational Safety and Health. (2010). *Best practices for dust control in coal mining.* Pittsburgh, Spokane.: Department of Health and Human Services.

Chao, W., & De-sheng, G. (2000). High-Efficiency Dust Scrubbers for Continous Miner in Underground Mines. *Journal of Central South University of Technology*, 204-211.

Colinet, J., Reed, W., & Potts, J. (2014). Continous Mining Dust Levels in 20- foot Cuts With and Without a Scrubber Operating. *SME Annual Meeting.* Salt Lake City: Society for Mining, Metallurgy, and Exploration, Littleton, Colorado.

Courtney, W. G. (n.d.). *The US Bureau of Mines program to control respirable dust in coal mines.* Pittsburgh: Bureau of Mines, US Department of the Interior.

Department of Labor, MSHA. (2014, May 1). *Lowering Miners' Exposure to Respirable Coal Mine Dust, Including Continuous Dust Monitors; Final Rule.* Retrieved February 12, 2016, from Federal Register, Vol 79, No. 84: http://arlweb.msha.gov/regs/fedreg/informationcollection/2014-09084.pdf

Gillies., A. (1982). Studies in Improvements to Coal Face Ventilation with Machine Mounted Dust Scrubber Systems. *SME -AIME Annual Meeting.* Dallas, Texas.: Society of Mining Engineers of AIME. Littleton, CO.

Kissell, F. N., & Goodman, G. V. (2003). Continuous miner and roof bolter dust control. In *Handbook for Dust Control in Mining* (pp. 23-38). Pittsburgh, PA: National Institute for Occupational Safety and Health.

Organiscak, J., & Beck, T. (2010). Continous Miner Spray Considerations for Optimizing Scrubber Performance in Exhaust Ventilation Systems. *Mining Engineering*, 41-46.

Wala, A., Vytla, S., Huang, G., & Taylor, C. (2008). Study of the Effects of Scrubber Operation on the Face Ventilation. *12th U.S./North American Mine Ventilation Symposium.* Reno, Nevada.